

NASA Technical Paper 1321

LOAN COPY: RETURN  
AFWL TECHNICAL LIB  
KIRTLAND AFB, N.



# Noise Transmission Through Flat Rectangular Panels Into a Closed Cavity

C. Kearney Barton and Edward F. Daniels

DECEMBER 1978

**NASA**



NASA Technical Paper 1321

Noise Transmission Through  
Flat Rectangular Panels  
Into a Closed Cavity

C. Kearney Barton and Edward F. Daniels  
*Langley Research Center*  
*Hampton, Virginia*



National Aeronautics  
and Space Administration

**Scientific and Technical  
Information Office**

1978

## SUMMARY

An experimental and analytical study was conducted on five panels backed by a closed cavity to determine the noise transmission characteristics of the coupled panel-cavity system. The closed cavity was studied both with and without fiber-glass lining to provide either an absorbent or a reverberant acoustic space. The effects on noise reduction of cavity absorption, measurement location within the cavity, panel mass, and panel stiffness were studied.

Results indicated that both measurement location and absorption in the cavity had significant effects on the noise reduction. Increasing panel mass improved the noise reduction at almost all frequencies, and increasing panel stiffness improved noise reduction below the fundamental resonance frequency. A simple, one-dimensional analytical model was developed which provided good agreement with the experimental results.

## INTRODUCTION

Several studies have shown that interior noise levels in light aircraft are high, partially due to the transmission of low-frequency propeller harmonics through the fuselage sidewall (refs. 1 to 6). Traditional noise-control techniques, such as added mass, absorption treatments, and/or double-wall construction, are inefficient at low frequencies (refs. 7 and 8). Other more advanced techniques, such as structural stiffening of fuselage skin and high leverage damping, have been investigated and show potential (refs. 9 and 10). However, these techniques have only been investigated in terms of transmission loss, which neglects the effects of the receiving acoustic space (aircraft cabin). The effects of the receiving space on noise transmission may be very important to the low-frequency noise transmission problem encountered in light aircraft.

In order to better understand the effects of the receiving space on low-frequency noise transmission, a rectangular box with one noise transmitting side was studied both experimentally and analytically. This model is analogous to the light aircraft where the noise transmitting side represents the aircraft sidewall and the cavity, or rectangular enclosure, represents the aircraft cabin.

Noise transmission through similar cavity-backed panels and its application to low-frequency noise transmission have been studied by several investigators (refs. 11 to 17). A review of the analytical work is presented in reference 17, along with a new analysis which extends previous work by calculating interior noise when only part of one side of the box transmits noise. As indicated in reference 17, considerable analytical work has been done on noise transmission through uniform panels into hard-wall cavities. Experimental results have also been limited to uniform panels and hard-wall cavities. Aircraft features that are important to the noise transmission and interior noise levels include stiff-

ness on the panels and absorptive material (fiber glass) on the inside of the panels. Review of the literature indicates that stiffening and absorption have not been studied in a situation that provides a clear indication of their effects at the low frequencies of interest here.

The purpose of this paper is to present results obtained from an experimental and theoretical study of the effects of stiffness and absorption on the transmission of noise through flat panels into a rectangular box. Noise reduction was studied for a variety of panels, both with and without fiber-glass lining in the cavity, for normally impinging sine waves and normally incident random noise. In order to provide insight into the effects of various system parameters and to make more tractable the mathematics associated with the soft-wall boundary condition, the analytical model was formulated as a flat plate of infinite length and width, located parallel to a wall whose surface impedance could be varied arbitrarily. Assumption of a plane, normally incident, acoustic wave reduced the analysis to one dimension. Both analytical and experimental results are examined to determine potential approaches to interior noise control.

#### SYMBOLS

A,B	constants of integration
c	speed of sound in air, m/s
$c_{fg}$	speed of sound in fiber glass, $c/1.18$ , m/s
f	frequency, Hz
$f_{11}$	panel fundamental frequency, Hz
$f_{mnq}$	frequency of $mnq$ cavity mode, Hz
h	fiber-glass thickness, m
j	$= \sqrt{-1}$
$K_C$	cavity stiffness, $\rho c^2/l$ , $N/m^3$
$K_p$	panel stiffness per unit area, $N/m^3$
k	wave number, $\omega/c$ , $m^{-1}$
l	cavity depth, $l = l_m$ , m
$l_m, l_n, l_q$	cavity dimensions, m
M	mass per unit area of panel (panel surface density), $kg/m^2$
m,n,q	cavity modal indices

NR	noise reduction, dB
P	fiber-glass porosity, 0.9
$p_i$	acoustic pressure inside cavity, $p_i(x)$ , $N/m^2$
$p_o$	acoustic pressure outside of cavity at panel surface, $N/m^2$
$R_{fg}$	flow resistivity of fiber glass, rayls/m (1 rayl = 1 $kg/(m^2\text{-sec})$ )
SPL	sound pressure level, dB
t	time, s
u	acoustic particle velocity, m/s
x	depthwise coordinate in cavity, m
$Z_c$	impedance of cavity at $x = 0$ , rayls
$Z_l$	impedance of fiber glass, rayls
$Z_p$	impedance of panel, $kg/m/s$
z	normalized fiber-glass impedance, $Z_l/\rho c$
$\zeta$	panel damping coefficient, percent
$\eta$	panel displacement, m
$\rho$	density of air, $kg/m^3$
$\rho_{fg}$	effective density of air in fiber glass, $\rho_{fg} = \rho$ , $kg/m^3$
$\phi$	$= (z - 1)/(z + 1)$
$\omega$	angular frequency, rad/s
$\omega_n$	angular natural frequency of panel, $2\pi f_{11}$ , rad/s
$\omega_n'$	angular natural frequency of panel including cavity effects, rad/s

Dot over symbol denotes time differentiation.

#### DESCRIPTION OF TEST APPARATUS

The apparatus used in the study is shown in figures 1 and 2. The test enclosure was mounted on soft rubber pads directly in front of two loudspeakers

which directed sound on the test panels. Sound transmitted through the test panels into the enclosure was measured and compared with the outside level to determine the sound transmission characteristics of each panel.

### Test Enclosure

The test enclosure was designed for high transmission loss through five sides with the sixth side left open for the mounting of test panels. As shown partially disassembled in figure 2(b), the enclosure basically consisted of two heavily framed, highly damped boxes mounted one inside the other by resilient mounts (natural frequency of 7 Hz). This construction was essentially a double-wall design. The walls of the inner box were 0.0025-m-thick aluminum, and the outer walls were 0.0032-m-thick aluminum. Each box wall was damped with a 0.0016-m-thick commercial damping material. The space between the two boxes was filled with 0.0127 m of acoustical absorptive foam, 0.0254 m of fiber glass, and about 0.06 m of empty airspace.

The interior dimensions of the inner box were 0.305 by 0.381 m, and the depth was 0.454 m. Tests were made both with the inner box empty, to provide a "hard wall" or reverberant condition, and with the inner box fiber glass lined, to provide a "soft wall" cavity or "dead" condition. The fiber-glass lining was 0.0254 m thick for each of the four sides adjacent to the open end, and 0.0762 m thick on the end opposite the opening. Test panels were mounted on the open side of the enclosure as shown in figure 2(a) and were clamped in place on the inner box. The gap between the two boxes (approximately 0.012 m) was sealed by using a commercial lead vinyl-foam composite having a surface density of about 5 kg/m<sup>2</sup>.

### Test Panels

The main physical characteristics of the five test panels used in the experiments are listed in table I. This group of panels was selected so that the effects of cavity, panel mass, and panel stiffness could be studied independently. Panel 1 was a limp, vinyl material that possessed no panel resonances; therefore, the only resonant behavior of the panel-cavity combination was due to the cavity effects. Panel 2 was a sheet of 0.0032-m-thick neoprene rubber and was also a limp, resonance-free panel. Panels 1 and 2 differed only in mass, each having essentially no stiffness, allowing for the investigation of the effects of panel mass on sound transmission. Panels 3, 4, and 5 were each 0.00079-m-thick aluminum; the difference between these three panels was the addition of stiffeners as shown in figure 3. Panel 3 had no stiffeners, panel 4 had four stiffeners in one direction, and panel 5 had stiffeners in both directions. Details of the stiffeners are shown in figure 4.

Panels 1, 3, 4, and 5 were used to investigate the effects of stiffness on noise transmission through the panels. These panels represent a large variation in stiffness, as indicated by the natural frequencies listed in table I. For example, panel 5 has a natural frequency (236 Hz) that is 4.2 times as

great as panel 3 (56 Hz), which implies a stiffness ratio of about 27 to 1 for these two panels. The corresponding change in mass is small (1.5 to 1) compared to the change in stiffness, so the differences in noise transmission characteristics are mainly due to differences in panel stiffness. The boundaries of each metallic panel (panels 3, 4, and 5) were grooved to simulate simple supports, but calculations for the simple-panel natural frequency later showed that the boundary conditions were closer to clamped.

The measured natural frequencies of each panel for two different conditions are listed in table I. First, the frequency was measured during the sound-transmission experiments. These frequencies were determined by maximizing the cavity sound pressure (which for the metallic panels corresponded to maximum panel displacement). The frequencies measured were the same for the hard-walled cavity and the fiber-glass lined cavity. Secondly, in order to approximate the "in vacuum" natural frequencies of the panels, one side of the box was removed while the test panels were in place so that air could escape from the cavity. The frequencies were then measured by determining the frequency where maximum panel displacement occurred.

#### Test Procedure

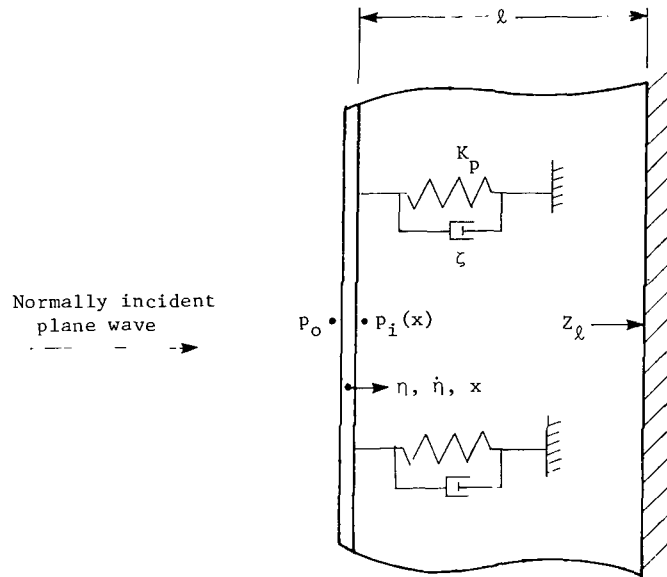
Each of the five test panels was tested with and without fiber-glass lining in the cavity for a total of 10 configurations. Noise reduction was measured for each configuration as a function of frequency using both sine wave and random excitation. In each test, four microphone locations were used. Two microphones were located inside the cavity directly behind the test panels as shown in figure 1. The other two microphones were located outside the enclosure about 0.01 m from the test panel as shown in figure 1.

Noise reduction measured for the sine wave excitation utilized a servocontrolled sweep oscillator with one outside microphone (location 1) as the control signal. The oscillator, which fed the amplifier speaker system, swept the frequency linearly at approximately 2 Hz/s from 40 to 1000 Hz while automatically adjusting its own output amplitude to maintain 110 dB SPL ( $\pm 1$  dB) at microphone location 1. The sound level inside the enclosure was recorded for each of the two locations as a continuous function of frequency. The difference between the inside and outside levels was the noise reduction.

When random excitation was used, the noise reduction was measured in a different manner. A random noise source (white noise) was input to the amplifier speaker system providing 120 dB SPL at each outside microphone. While maintaining this level, a one-third-octave analysis was performed on the signals from each of the four microphones. The real-time one-third-octave analysis was performed with a parallel filter system using an 8-s integration time. Noise reduction was determined by energy averaging the two outside sound pressure levels in each one-third-octave band and then subtracting the corresponding band for each inside microphone. Thus, there resulted a noise-reduction curve as a function of the standard one-third-octave center frequencies from 40 to 10 000 Hz.

## ANALYSIS

The model used in the analytical study is shown in the following sketch:



The model consists of an infinite, rigid wall connected by springs and dash pots to the ground. The infinite wall behind the panel has complex impedance  $Z_l$ . With a normal incidence plane wave, this system represents a one-dimensional problem where the panel is a single-degree-of-freedom (SDOF) oscillator and the acoustic space behind the panel includes all one-dimensional acoustic modes.

The equation of motion for the panel in terms of impedances is

$$p_o = \dot{\eta} Z_p + \dot{\eta} Z_c \quad (1)$$

where  $Z_p$  is the SDOF panel impedance

$$Z_p = 2\zeta\omega_n M + j\left(\omega M - \frac{K_p}{\omega}\right) \quad (2)$$

and  $Z_c$  is the impedance of the cavity at the panel.

The wave equation for the one-dimensional acoustic space is

$$\frac{\partial^2 p_i}{\partial x^2} = \frac{1}{c^2} \frac{\partial^2 p_i}{\partial t^2} \quad (3)$$



The boundary conditions for the acoustic space are

$$u = \dot{\eta} \quad (x = 0) \quad (4)$$

and

$$\frac{p_i}{u} = Z_l \quad (x = l) \quad (5)$$

where  $u$  is the acoustic particle velocity and is related to pressure by the momentum equation. A solution for  $p_i$  is assumed in the form

$$p_i = A \exp[j(\omega t - kx)] + B \exp[j(\omega t + kx)] \quad (6)$$

where  $A$  and  $B$  are constants to be found using the boundary conditions. Imposing the boundary conditions and solving for  $A$  and  $B$  gives the solution for  $p_i$  as

$$p_i = \dot{\eta} \rho c \left[ \frac{\exp(j2kl) + \phi}{\exp(j2kl) - \phi} \cos kx - j \sin kx \right] \quad (7)$$

where

$$\phi = \frac{Z_l - \rho c}{Z_l + \rho c} \quad (8)$$

By solving for  $p_i/\dot{\eta}$  and setting  $x = 0$ ,  $Z_{\text{cavity}}$  can be determined from equation (7) as

$$Z_c = \rho c \frac{Z_l + j\rho c \tan kl}{\rho c + jZ_l \tan kl} \quad (9)$$

Solving equation (1) for  $\dot{\eta}$  and substituting the result into equation (7) results in

$$p_i = p_o \left( \frac{\rho c}{Z_p + Z_c} \right) \left[ \frac{\exp(j2kl) + \phi}{\exp(j2kl) - \phi} \cos kx + j \sin kx \right] \quad (10)$$

The noise reduction NR is defined by

$$NR = -20 \log \frac{|P_i|}{|P_o|} \quad (11)$$

and can be calculated by using equations (2), (8), (9), (10), and (11) as a function of  $Z_p$ ,  $Z_l$ ,  $l$ ,  $x$ , and  $f$ .

The impedance  $Z_p$  can be found from equation (2) where  $\zeta$  is the damping coefficient (estimated to be 2 percent),  $M$  is the surface density, and  $\omega_n$  is the panel natural frequency in a vacuum approximated by measuring the natural frequency with one side of the cavity open (table I). Since the panel was assumed to be an SDOF system,  $K_p$  may be determined from  $\omega_n = \sqrt{K_p/M}$  as

$$K_p = \omega_n^2 M$$

The fiber-glass impedance  $Z_l$  was taken from reference 18 and, in the notation of the present paper, is

$$Z_l = \frac{\rho_{fg}}{\sqrt{P}} \left( 1 - j \frac{R_{fg}}{\rho_{fg}\omega} \right)^{1/2} \coth \left[ j \frac{\omega \sqrt{P}}{c_{fg}} \left( 1 - j \frac{R_{fg}}{\rho_{fg}\omega} \right)^{1/2} h \right] \quad (12)$$

Equation (12) was derived for the normal acoustic impedance of isotropic porous materials with thickness  $h$  and backed by a rigid wall. The flow resistivity  $R_{fg}$  was found from figure 10.4 of reference 7 and is 20 000 mks rayls/m. This value was determined from reference 7 by using the fiber-glass density which was measured to be 49 kg/m<sup>3</sup> and a fiber size which was assumed to be 0.008 mm.

For very low frequencies, equations (2), (8), (9), (10), and (11) may be combined to show that NR approaches a constant (independent of frequency) as follows:

$$\lim_{f \rightarrow 0} NR = 20 \log \left( \frac{K_C + K_p}{K_C} \right) \quad (13)$$

where  $K_C = \frac{\rho c^2}{l}$  and  $K_C$  is the stiffness per unit area provided by the cavity to the panel. Thus, for  $K_C < K_p$ , NR increases at 6 dB per doubling of  $K_p/K_C$ ; this result was also found by previous investigators (refs. 11 and 14).

For panel-cavity systems without fiber glass and for low frequencies where  $k\ell \ll 1$ , it may be shown that the coupled panel-cavity resonance is slightly higher in frequency than the panel alone; that is,

$$\omega_n' \approx \sqrt{\omega_n^2 + \frac{\rho c^2}{\ell M}} = \sqrt{\frac{K_p + K_c}{M}} \quad (14)$$

Equation (14) is the frequency where  $Z_p + Z_c$  is minimized (eq. (10)) and shows that the cavity adds stiffness to the panel. The measured natural frequencies for panels 1, 2, and 3 in table I demonstrate this effect.

## RESULTS AND DISCUSSION

The noise reduction of a panel-cavity system is dependent on two factors: cavity effects and panel effects. These effects are described separately in the following sections, with analytical and experimental results presented together.

### Effects of Cavity on Noise Reduction

Figure 5 shows the measured and theoretical noise reduction for two interior microphone locations. A sine wave input was used, the cavity was hard walled, and the panel used was of polyvinylchloride (PVC), panel 1 in table I. This panel was used to help isolate the cavity effects due to the nonresonant mass behavior of the PVC. The variation in noise reduction with frequency is readily apparent. It should be noted that noise reduction is dependent on measurement location in the cavity at some frequencies. For example, there is a 15-dB difference in NR at 500 Hz for the two microphone locations (figs. 5(a) and 5(b)).

Figure 5 also indicates that the results of theoretical noise reduction agree reasonably well with the measured noise reduction. Some differences between theory and experiment occur at the depthwise cavity modes and nodal points. This was expected because there is some acoustic damping due to various mechanisms that are not included in the theory, as well as some acoustic leakage through the enclosure sides. Another discrepancy in the data is at the two cross cavity modes, which are indicated as  $f_{020}$  and  $f_{120}$  in figure 5(a). These modes were identified by comparing the frequencies in figure 5(a) to the acoustic modes in table II which are for a hard-walled, rectangular enclosure. Cross modes are those having nonzero  $n$  or  $q$  in table II. The reason that only two cross modes ( $n = z$ ) were observed is probably because the other modes ( $n = 1$ ) have nodal points at the center where the microphones were located.

Figure 6 shows the effect of fiber-glass lining in the cavity on noise transmission by comparing NR for the same PVC panel for the hard-wall and soft-wall cavities. (Fig. 6(a) is the same as fig. 5(a).) Comparison of the results shows that fiber glass reduces the modal response of the cavity and

essentially eliminated all cavity modes except the first depthwise mode. The analytical model predicts the noise reduction well, except at the panel-cavity resonance. The relatively small cross-mode response of the lined cavity suggests that the one-dimensional assumption is sufficient for absorbent cavities.

An additional point to note in the comparison is the large change in frequency of the first cavity resonance, from 392 to 344 Hz. This frequency shift corresponds to about 34 percent critical damping for a single-degree-of-freedom oscillator ( $\omega_n' = \omega_n \sqrt{1 - 2\zeta^2}$ ).

### Effects of Panel Dynamics

The panel dynamical quantities discussed in this paper are panel stiffness and panel mass.

Panel mass.— Figure 7 shows the effects of mass on noise reduction by comparing NR for two panels having different mass and the same stiffness. The panels used were panel 1 and panel 2 in table I. Both panels had essentially no stiffness. The fiber-glass lined cavity was used to minimize cavity effects.

Both theoretical (fig. 7(a)) and experimental (fig. 7(b)) results showed about a 4 dB improvement with the heavier panel at essentially all frequencies. This improvement can be calculated by the classical mass law relationship.

One exception to the improvement provided by additional mass is at the system resonance. The system resonance is shifted because of the increased mass while constant stiffness is provided by the cavity  $\left(K_c - \frac{\rho c^2}{l}\right)$ .

Panel stiffness.— Figure 8 shows the theoretical effects of panel stiffness, with other quantities held constant. Curves are shown for three hypothetical panels having natural frequencies of 100, 200, and 1000 Hz. Because the theoretical model assumes a single-degree-of-freedom panel, stiffness is proportional to natural frequency squared ( $K_p = \omega_n^2 M$ ).

The results show that increasing panel stiffness (or raising the natural frequency) substantially improves NR at frequencies below panel resonance. The amount of improvement at very low frequencies is analogous to mass law

$$\Delta NR = 20 \log \frac{(K_p)_2}{(K_p)_1} = 40 \log \frac{(\omega_n)_2}{(\omega_n)_1}$$

where the subscript 2 represents a stiffened panel and the subscript 1 represents the original panel. Above panel resonance, the curves quickly converge. Thus, increasing stiffness theoretically improves NR at low frequencies below the panel natural frequency.

Results demonstrating the effects of increasing panel stiffness are shown in figure 9. The cavity was again lined with fiber glass to minimize the effects of the cavity. The noise reduction shown in figure 9 is for two aluminum panels having different natural frequencies (panels 3 and 5 in table I). The double stiffened panel (panel 5, table I) had approximately 50 percent greater mass than the simple panel (panel 3, table I) but had approximately 27 times more stiffness (for the fundamental mode). The data show that the stiffer panel (fig. 9(b)) generally provides greater NR at frequencies below the panel fundamental. Above the fundamental frequency, the data indicate resonant panel behavior. The theoretical model, however, assumed only one panel resonance and, hence, does not predict this resonant behavior.

When NR is expressed in one-third-octave bands for a random noise input, the panel resonances above the fundamental frequency average out as indicated in figure 10. This figure shows the measured and calculated NR for four panels (panels 1, 3, 4, and 5 in table I) with the fiber-glass lined cavity. This group of panels represents a large variation in stiffness with a relatively small change in mass. Figure 10 shows that increasing the panel natural frequency (and hence its stiffness) increases NR below the first panel resonance (denoted  $f_{11}$  in fig. 10).

As previously mentioned, the higher panel modes are not resolved because of the one-third-octave bandwidth, and only the fundamental panel mode has a significant effect on the measured noise reduction. The second dip in the noise-reduction curves in figure 10 is from the first cavity mode at about 350 Hz. These results suggest that the single-panel-mode, one-dimensional model is adequate for predicting NR in one-third-octave bands with random noise inputs for an absorbent cavity.


#### SUMMARY OF RESULTS

An analytical and experimental investigation of noise reduction through a panel backed by a closed cavity was conducted. The effects on noise reduction of fiber-glass lining, location in the cavity, panel mass, and panel stiffness were investigated for sine wave input and random input.

The one-dimensional theory predicted the measured noise reduction reasonably well for the two limp panels, both with and without fiber-glass lining in the cavity. The theory worked very well for the fiber-glass lined cavity.

Theoretical and experimental data showed an important relationship between noise reduction and measurement location in the cavity, and the two measurement locations resulted in a 15-dB difference in noise reduction at a particular frequency.

Increasing panel mass for limp panels provided an improvement in noise reduction at almost all measured frequencies, and the improvements generally obeyed mass law. Increasing panel stiffness, or natural frequency, improved noise reduction only below the fundamental resonance frequency.



Sine wave excitation of the aluminum panels showed that panel modes above the fundamental have a significant effect on the noise reduction. However, results from the same panels excited by random noise showed that only the first panel resonance has a significant effect on the one-third-octave band noise reduction, thus indicating that the single-panel-mode analytical model described herein is sufficient for such cases.

Langley Research Center  
National Aeronautics and Space Administration  
Hampton, VA 23665  
October 18, 1978

## REFERENCES

1. Tobias, Jerry V.: Noise in Light Twin-Engine Aircraft. Sound & Vib., vol. 3, Sept. 1969, pp. 16-19.
2. Gilbert, Gordon: Cabin Noise Levels. Bus. & Commer. Aviat., July 1976, pp. 80-82, 84, 86.
3. Mixson, John S.; Barton, C. Kearney; and Vaicaitis, Rimas: Investigation of Interior Noise in a Twin-Engine Light Aircraft. J. Aircr., vol. 15, no. 4, Apr. 1978, pp. 227-233.
4. Catherines, John J.; and Mayes, William H.: Interior Noise Levels of Two Propeller-Driven Light Aircraft. NASA TM X-72716, 1975.
5. Morgan, Homer G.: Trends in Aircraft Noise Alleviation. Vehicle Technology for Civil Aviation - The Seventies and Beyond, NASA SP-292, 1971, pp. 301-315.
6. Wick, Robert L., Jr.; Roberts, Lester B.; and Ashe, William F.: Light Aircraft Noise Problems. Aerosp. Medicine, vol. 34, no. 12, Dec. 1963, pp. 1133-1137.
7. Beranek, Leo L., ed.: Noise and Vibration Control. McGraw-Hill Book Co., Inc., c.1971.
8. Harris, Cyril M., ed.: Handbook of Noise Control. McGraw-Hill Book Co., Inc., c.1957.
9. Getline, G. L.: Low-Frequency Noise Reduction of Lightweight Airframe Structures. NASA CR-145104, 1976.
10. SenGupta, G.: Methods of Reducing Low Frequency Cabin Noise and Sonically Induced Stresses, Based on the Intrinsic Structural Tuning Concept. AIAA Paper No. 77-444, Mar. 1977.
11. Lyon, Richard H.: Noise Reduction of Rectangular Enclosures With One Flexible Wall. J. Acoust. Soc. America, vol. 35, no. 11, Nov. 1963, pp. 1791-1797.
12. Vaicaitis, Rimas; and McDonald, Wayne: Noise Transmission Into an Enclosure. Advances in Civil Engineering Through Engineering Mechanics, American Soc. Civil Eng., c.1977, pp. 128-131.
13. Vaicaitis, Rimas: Noise Transmission by Viscoelastic Sandwich Panels. NASA TN D-8516, 1977.
14. Guy, R. W.; and Bhattacharya, M. C.: The Transmission of Sound Through a Cavity-Backed Finite Plate. J. Sound & Vib., vol. 27, no. 2, Mar. 1973, pp. 207-223.

15. Pretlove, A. J.: Forced Vibrations of a Rectangular Plate Backed by a Closed Rectangular Cavity. *J. Sound & Vib.*, vol. 3, no. 3, May 1966, pp. 252-261.
16. Gorman, George F., III: Random Excitation of a Panel-Cavity System. AMS Rep. No. 1009 (NASA Grant NGR 31-001-146), Princeton Univ., July 1971. (Also available as NASA CR-112051.)
17. McDonald, Wayne B.; Vaicaitis, Rimas; and Myers, Michael K.: Noise Transmission Through Plates Into an Enclosure. NASA TP-1173, 1978.
18. Beranek, Leo L.: Acoustic Impedance of Porous Materials. *J. Acoust. Soc. America*, vol. 13, no. 3, Jan. 1942, pp. 248-260.



TABLE I.- PHYSICAL CHARACTERISTICS OF TEST PANELS

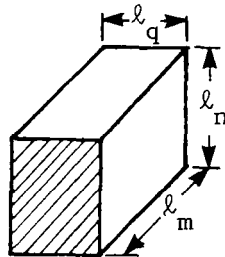
Panel	Material	Thickness, h, mm	Surface density, M, kg/m <sup>2</sup>	Stiffeners	Measured natural frequency, Hz	
					With cavity	Without cavity
1	PVC <sup>a</sup>	1.6	2.50	None	50	0
2	Rubber	3.2	3.96	None	45	0
3	Aluminum	.79	2.17	None	76	56
4	Aluminum	.79	2.69	One direction	170	170
5	Aluminum	.79	3.30	Two directions	232	236

<sup>a</sup>Lead impregnated polyvinylchloride.

TABLE II.- HARD-WALL CAVITY MODES

$$f_{mnq} = \frac{c}{2} \sqrt{\left(\frac{m}{l_m}\right)^2 + \left(\frac{n}{l_n}\right)^2 + \left(\frac{q}{l_q}\right)^2}; \quad l_m = 0.454 \text{ m};$$

$$l_n = 0.381 \text{ m}; \quad l_q = 0.305 \text{ m}; \quad c = 348 \text{ m/s}$$



Modal number			Calculated frequency, $f_{mnq}$ , Hz
m	n	q	
0	0	0	0
1	0	0	383
0	1	0	457
0	0	1	571
1	1	0	596
1	0	1	688
0	1	1	731
2	0	0	766
1	1	1	825
2	1	0	892
0	2	0	913
2	0	1	956
1	2	0	991

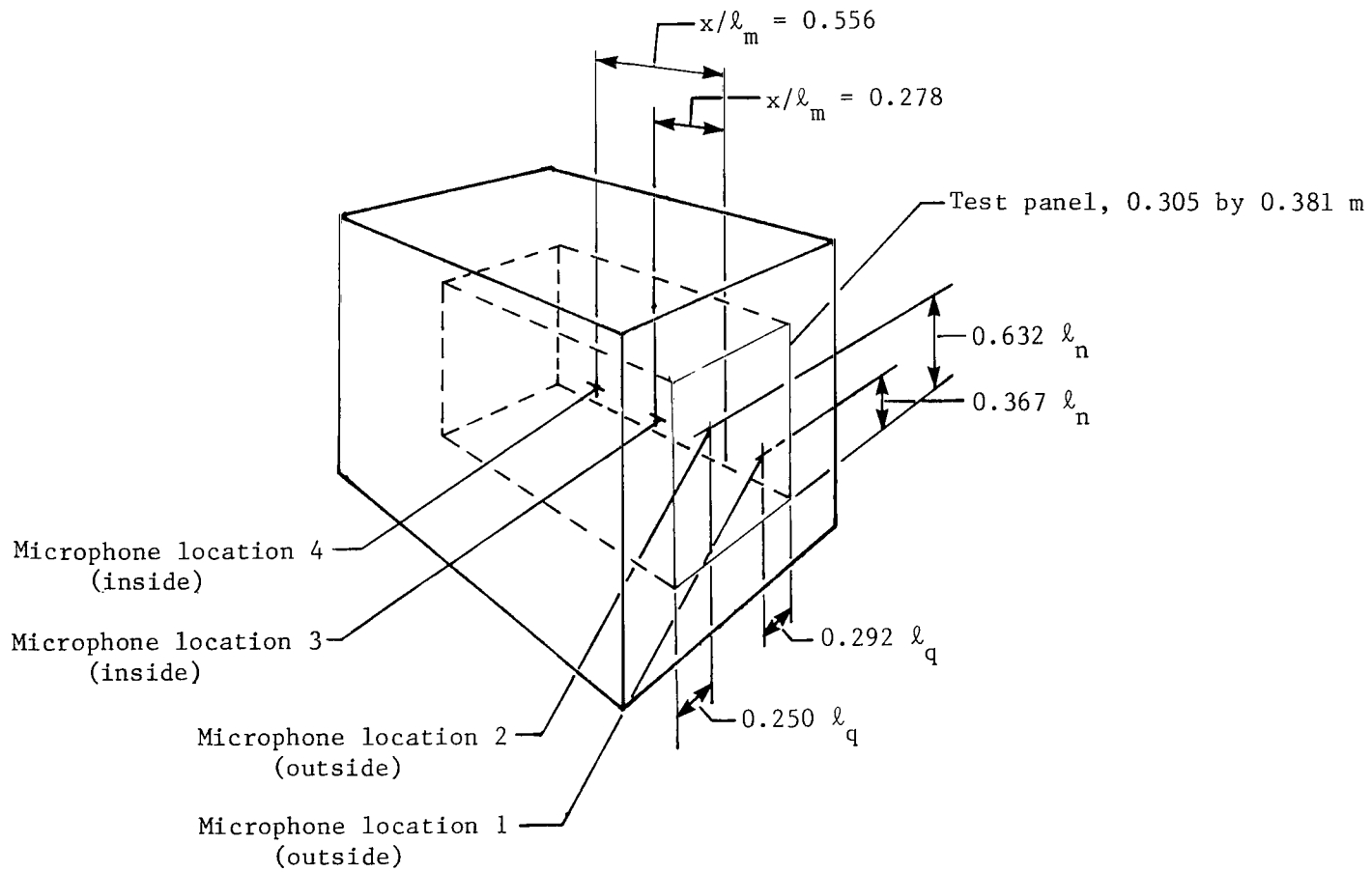
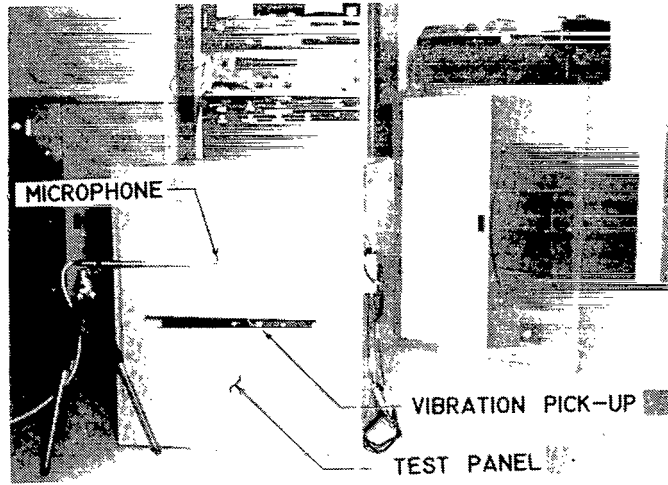
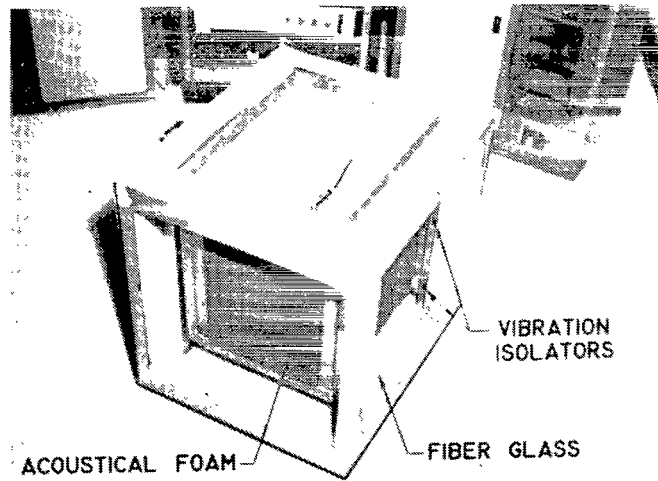


Figure 1.- Test enclosure.

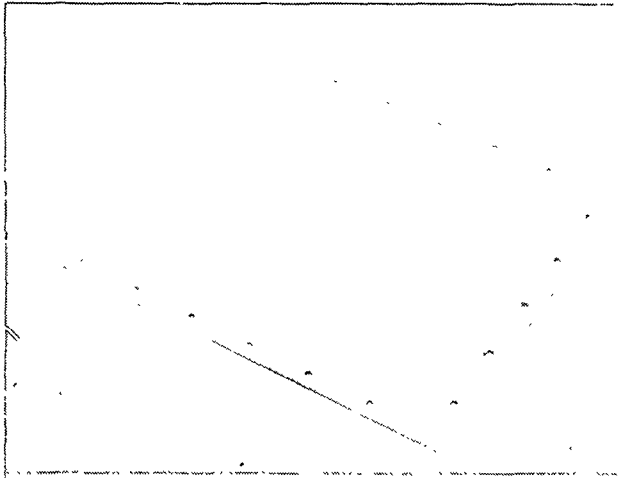


(a) Sound-proof enclosure.

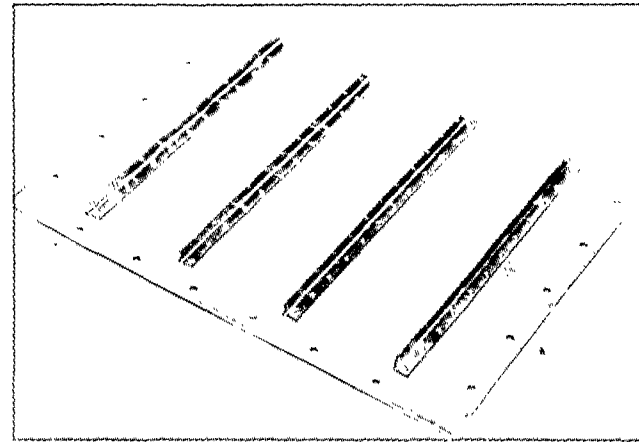


(b) Partially disassembled enclosure showing design features.

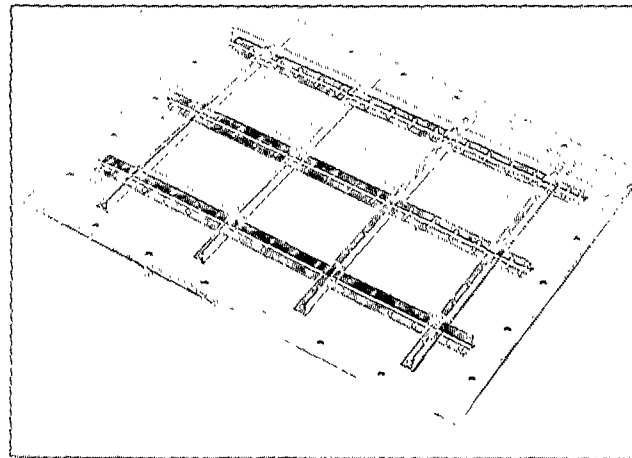
Figure 2.- Noise-reduction test apparatus. L-78-147



(a) Panel 3 without stiffeners  
(panels 1 and 2 similar).



(b) Panel 4 with stiffeners in  
one direction.



(c) Panel 5 with stiffeners in  
two directions.

L-78-148

Figure 3.- Noise-reduction test panels.

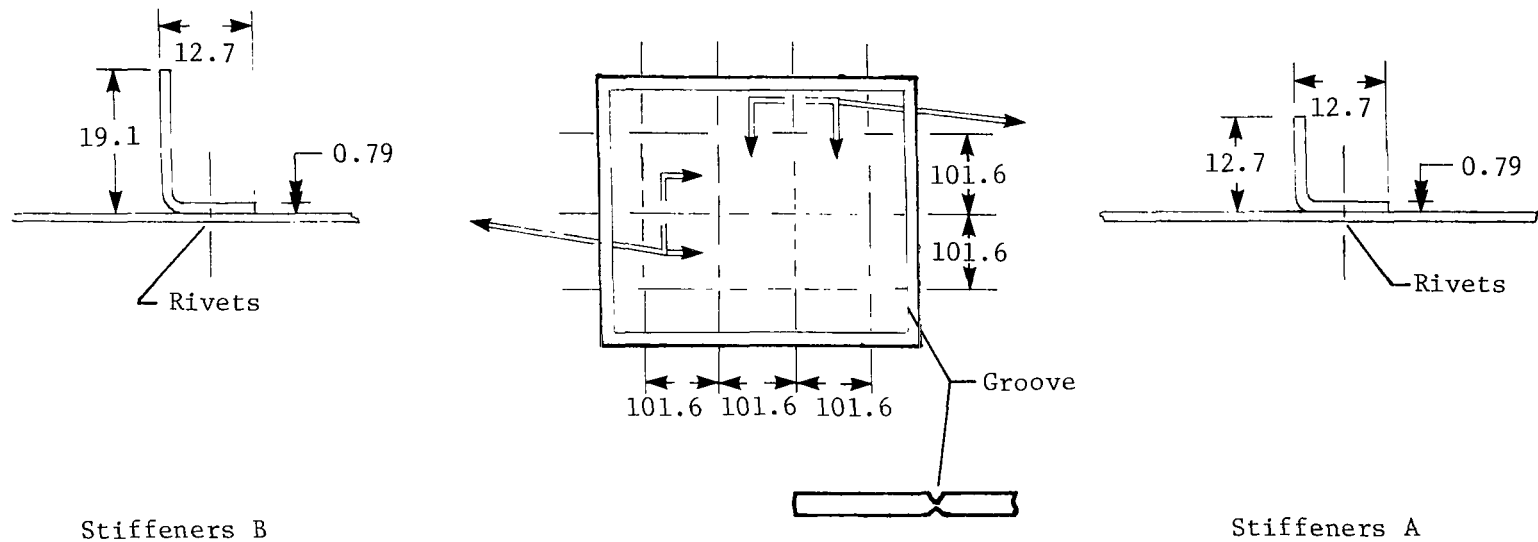
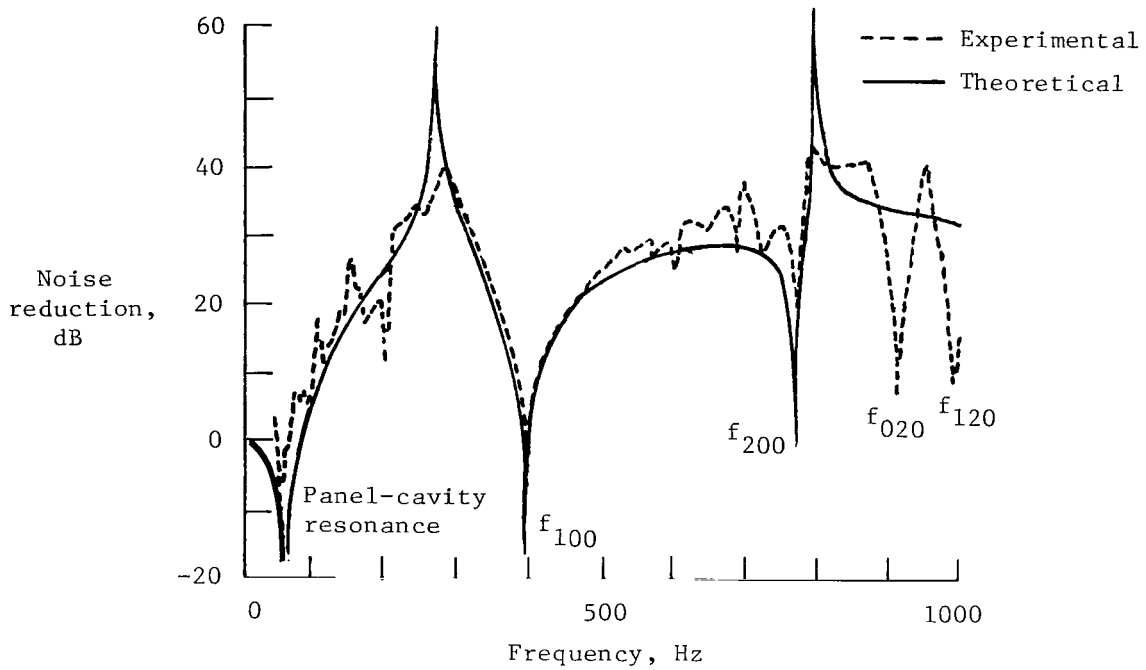
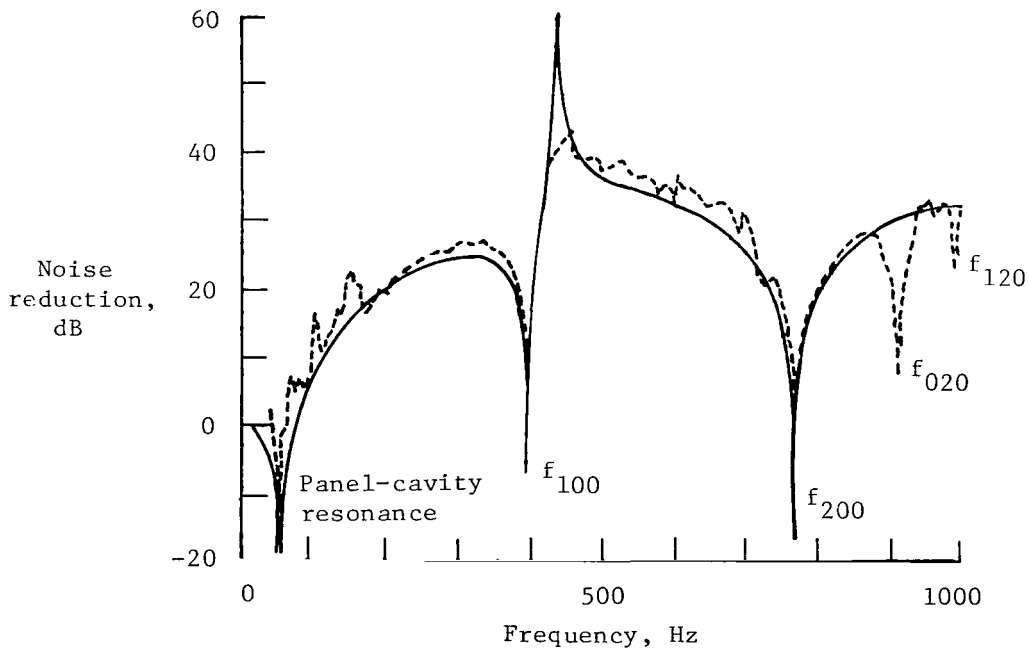


Figure 4.- Details of panel stiffeners. (Stiffeners A used on panels 4 and 5; stiffeners B used on panel 5.) All dimensions are in mm; rivets are spaced 25.4 mm apart.

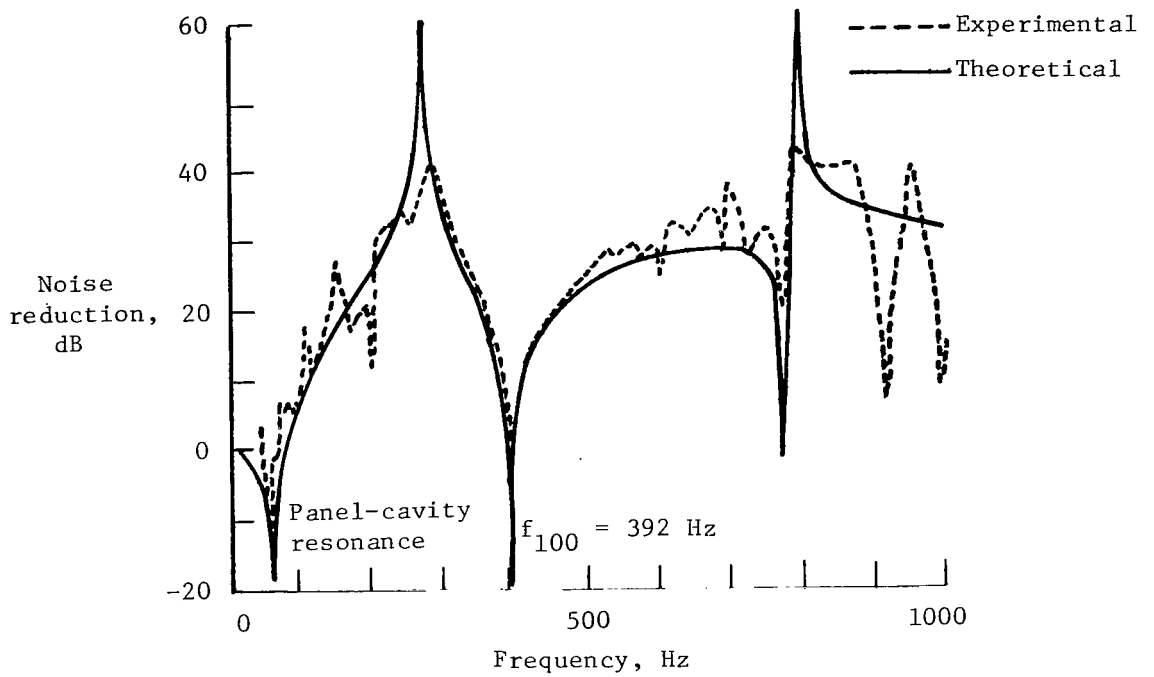


(a) Microphone location 3.  $x/l = 0.278$ .

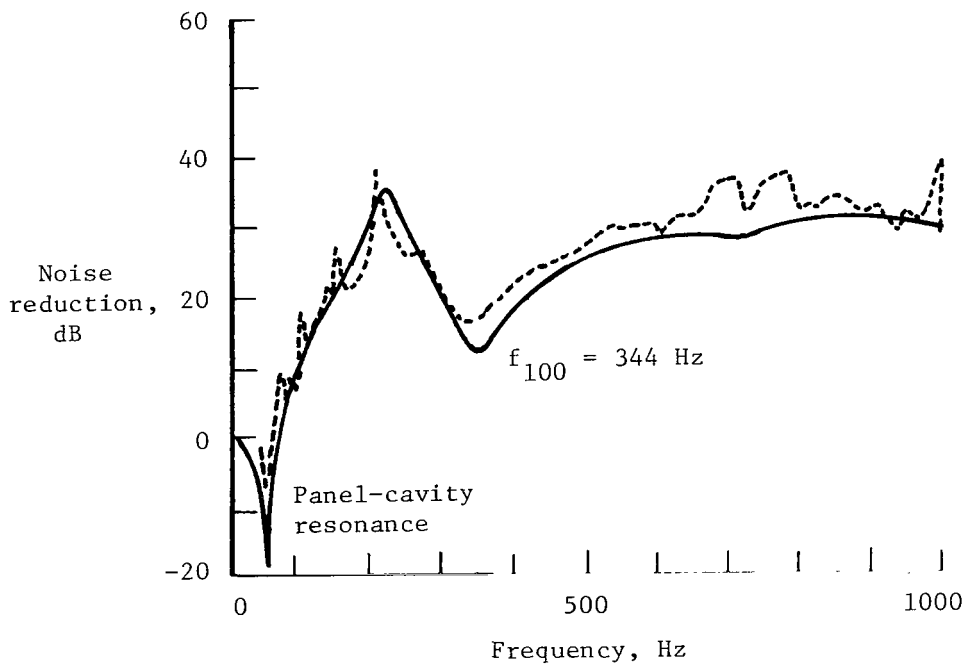


(b) Microphone location 4.  $x/l = 0.556$ .

Figure 5.- Effect of microphone location on noise reduction for panel 1 (table I). Panel-cavity resonance from equation (9).



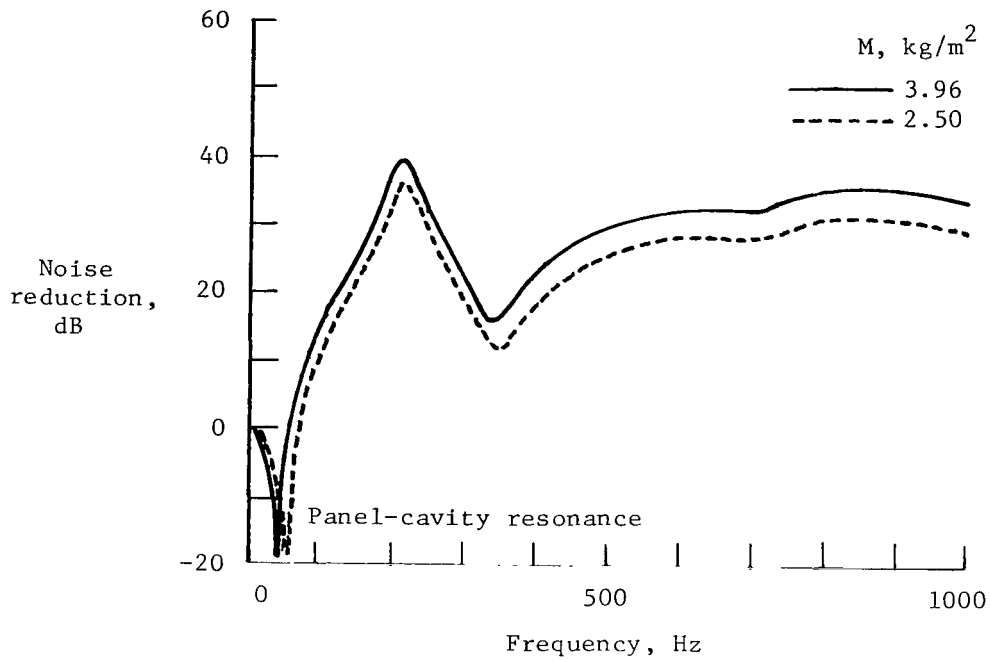
(a) Hard-wall cavity.



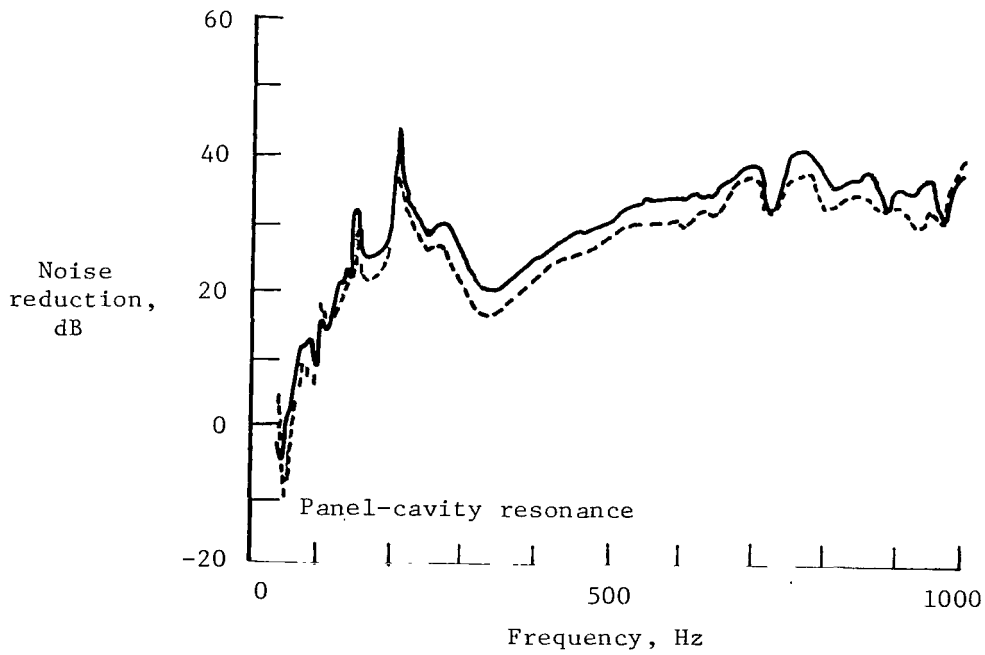
(b) Fiber-glass lined cavity.

Figure 6.- Effect of fiber glass on noise reduction for panel 1 (table I). Microphone location 3;  $x/l = 0.278$ ; panel-cavity resonance from equation (9).





(a) Theoretical.



(b) Experimental.

Figure 7.- Effect of mass on noise reduction for fiber-glass lined cavity.  $x/l = 0.278$ ; panel-cavity resonance from equation (9).

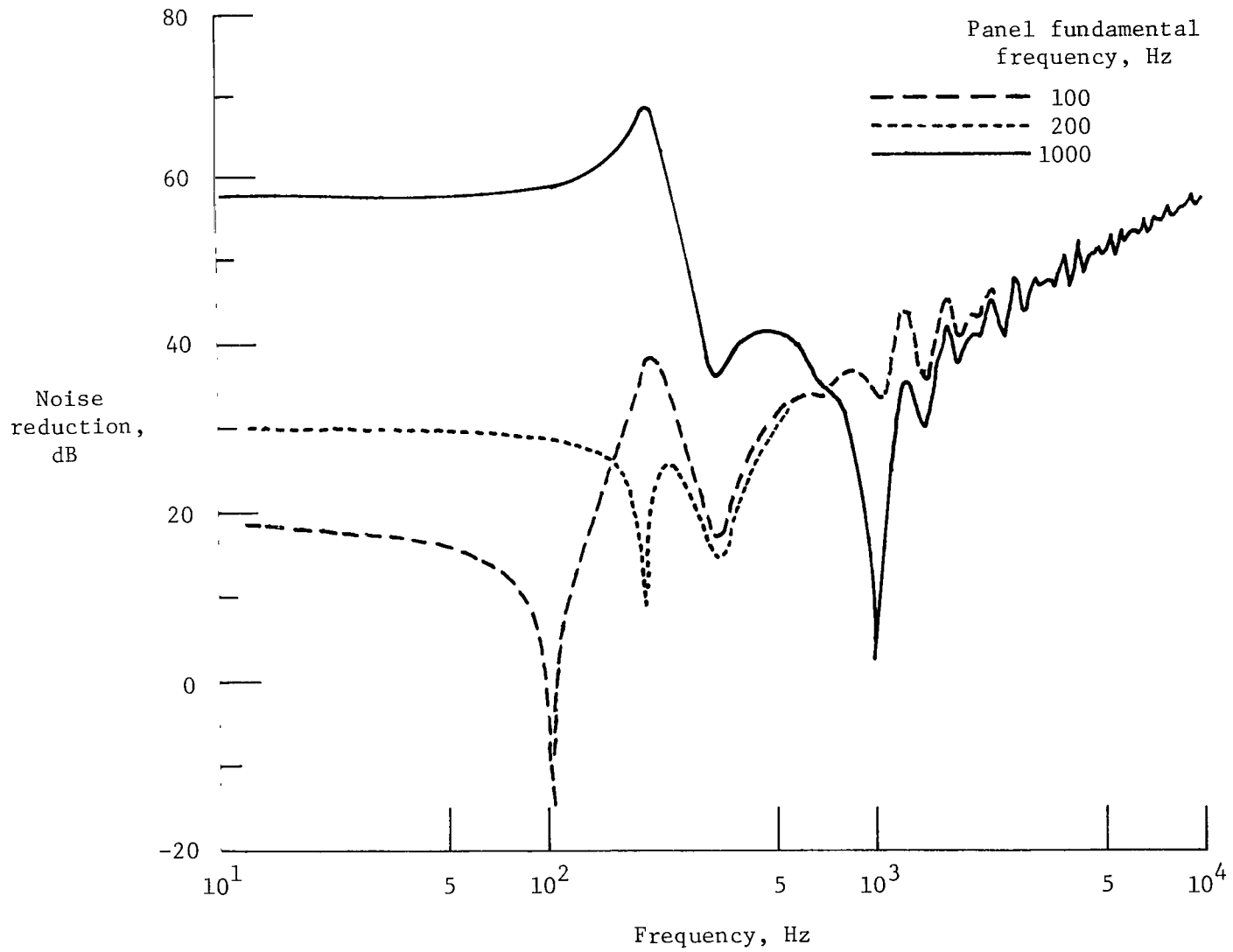
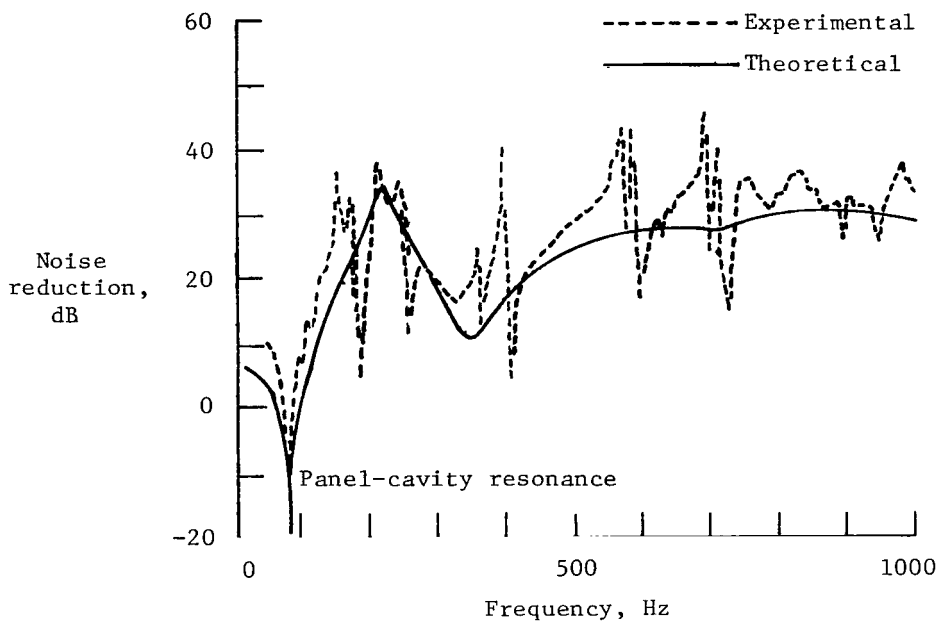
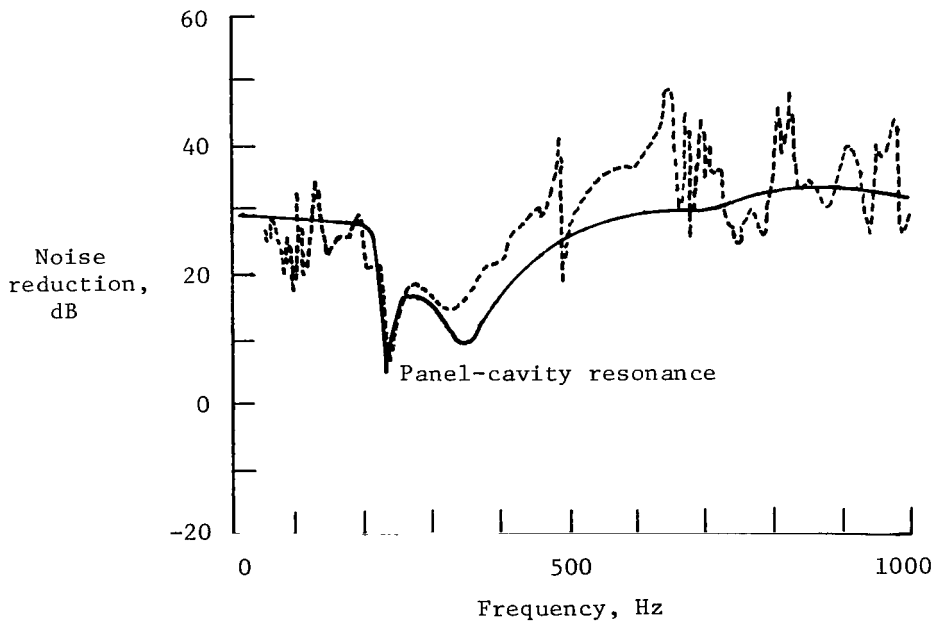


Figure 8.- Theoretical effect of panel stiffness on noise reduction for fiber-glass lined cavity.  $M = 5 \text{ kg/m}^2$ ;  $x/l = 0.278$ .



(a) Simple panel (panel 3, table I).  $f_{11} = 56$  Hz.



(b) Double stiffened panel (panel 5, table I).  $f_{11} = 236$  Hz.

Figure 9.- Experimental and theoretical effects of panel stiffness on noise reduction for fiber-glass lined cavity.  $x/l = 0.278$ ; panel-cavity resonance from equation (9).

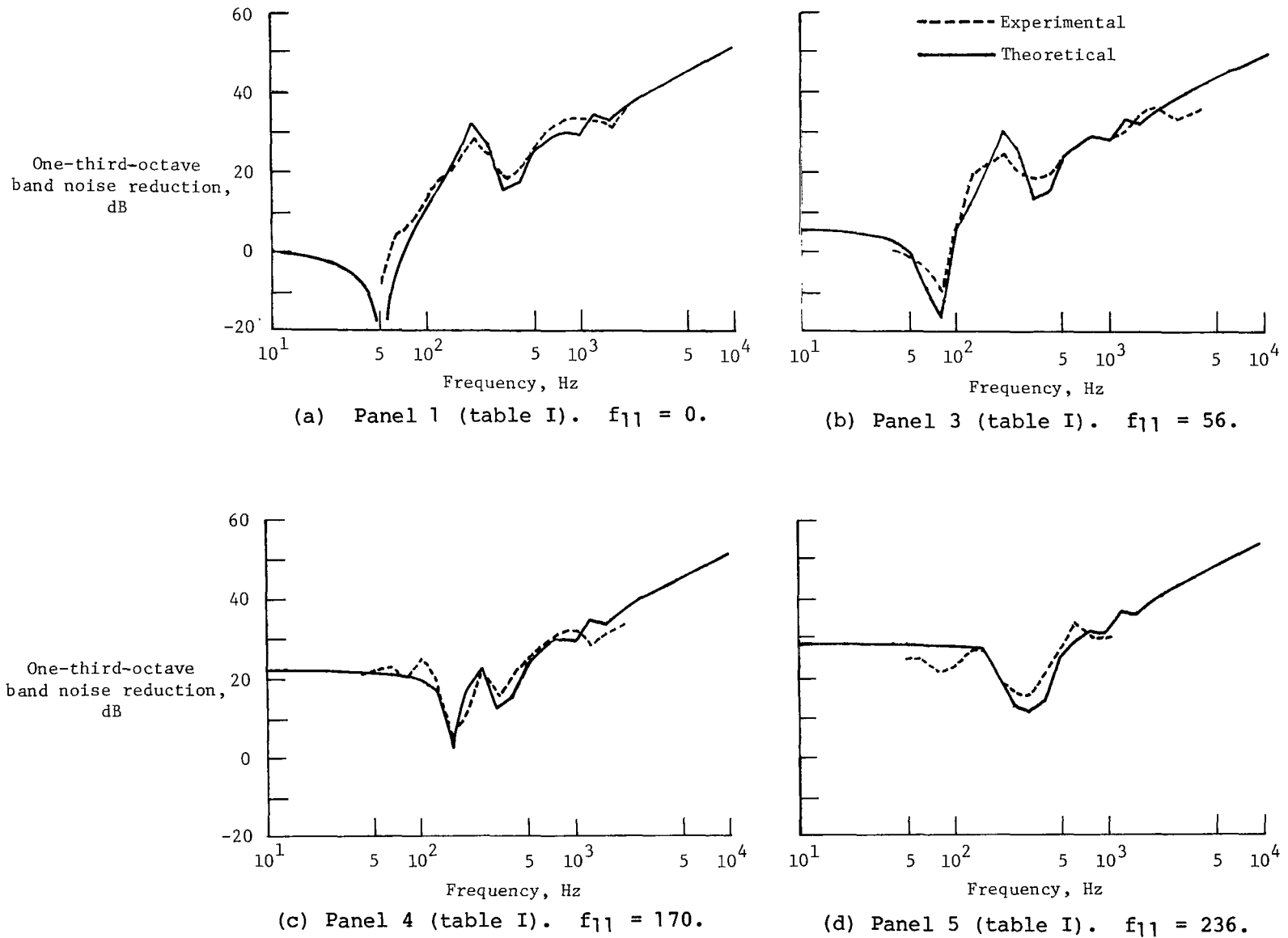


Figure 10.- Effect of stiffness on one-third-octave band noise reduction for fiber-glass lined cavity.  $x/l = 0.278$ .

1. Report No. NASA TP-1321		2. Government Accession No.		3. Recipient's Catalog No.	
4. Title and Subtitle NOISE TRANSMISSION THROUGH FLAT RECTANGULAR PANELS INTO A CLOSED CAVITY				5. Report Date December 1978	
7. Author(s) C. Kearney Barton and Edward F. Daniels				6. Performing Organization Code	
9. Performing Organization Name and Address NASA Langley Research Center Hampton, VA 23665				8. Performing Organization Report No. L-12439	
12. Sponsoring Agency Name and Address National Aeronautics and Space Administration Washington, DC 20546				10. Work Unit No. 505-09-23-01	
15. Supplementary Notes				11. Contract or Grant No.	
16. Abstract  An experimental and analytical study was conducted on five panels backed by a closed cavity to determine the noise transmission characteristics of the coupled panel-cavity system. The closed cavity was studied both with and without fiberglass lining to provide either an absorbent or a reverberant acoustic space. The effects on noise reduction of cavity absorption, measurement location within the cavity, panel mass, and panel stiffness were studied. A simple, one-dimensional analytical model was developed which provided good agreement with the experimental results.				13. Type of Report and Period Covered Technical Paper	
17. Key Words (Suggested by Author(s)) Panel stiffness and mass Cavity absorption Low-frequency noise reduction Cavity-backed panel				14. Sponsoring Agency Code	
18. Distribution Statement Unclassified - Unlimited				Subject Category 71	
19. Security Classif. (of this report) Unclassified		20. Security Classif. (of this page) Unclassified		21. No. of Pages 26	22. Price* \$4.50

\* For sale by the National Technical Information Service, Springfield, Virginia 22161

NASA-Langley, 1978

National Aeronautics and  
Space Administration

THIRD-CLASS BULK RATE

Postage and Fees Paid  
National Aeronautics and  
Space Administration  
NASA-451



Washington, D.C.  
20546

Official Business  
Penalty for Private Use, \$300

3 1 1U,H, 121278 S00903DS  
DEPT OF THE AIR FORCE  
AF WEAPONS LABORATORY  
ATTN: TECHNICAL LIBRARY (SUL)  
KIRTLAND AFB NM 87117

S

**NASA**

POSTMASTER: If Undeliverable (Section 158  
Postal Manual) Do Not Return